Physica Medica 140 (2025) 105684

Contents lists available at ScienceDirect

Physica Medica

journal homepage: www.elsevier.com/locate/ejmp

Original paper

Improvements of lateral penumbra at various depth regions in proton pencil beam scanning with a multileaf collimator: Dose verifications and plan comparisons

Yuki Tominaga [a,b,*], Yushi Wakisaka [a,b], Takahiro Kato [c,d], Keisuke Yasui [e], Ryohei Kato [d], Masaya Ichihara [b,f], Masashi Tomida [f], Motoharu Sasaki [g], Masataka Oita [h], Teiji Nishio [b]

[a] Department of Radiotherapy, Medical Co. Hakuhokai, Osaka Proton Therapy Clinic, 27-9 Kasugadenaka 1 Chome, Konohana-ku, Osaka, Osaka 554-0022, Japan
[b] Medical Physics Laboratory, Division of Health Science, Graduate School of Medicine, The University of Osaka, 1-7 Yamadaoka, Suita-Shi, Osaka 565-0871, Japan
[c] Department of Radiological Sciences, School of Health Sciences, Fukushima Medical University, 10-6 Sakae-machi, Fukushima 960-8516, Japan
[d] Department of Radiation Physics and Technology, Southern Tohoku Proton Therapy Center, 172, Yatsuyamada 7 Chome, Koriyama, Fukushima 963-8052, Japan
[e] School of Medical Sciences, Fujita Health University, 1-98 Dengakugakubo, Kutsukake-cho, Toyoake, Aichi 470-1192, Japan
[f] Department of Proton Beam Technology Room, Narita Memorial Proton Center, 78 Shirakawa-cho, Toyohashi, Aichi 441-8021, Japan
[g] Graduate School of Biomedical Sciences, Tokushima University, 3.-8-5 Kuramoto-cho, Tokushima, Tokushima 770-8503, Japan
[h] Faculty of Interdisciplinary Science and Engineering in Health Systems, Okayama University, 5-1 Shikata-cho, 2-chome, Kita-ku, Okayama, Okayama 700-8558, Japan

ARTICLE INFO

Keywords:
Proton therapy
Pencil beam scanning
Multileaf collimator
Lateral penumbra
Treatment planning

ABSTRACT

Purpose: In scanned proton therapy, the current consensus is that the effective range of the collimator's contribution to lateral penumbra improvement is up to approximately 150 mm depth. We characterized the penumbra variations for scanned proton beams with or without a new type of multileaf collimator (MLC) under various air gaps, depth, and with or without range shifter (RS).

Methods: Eighty-six uniform dose plans were created (38 RS-negative and 48 RS-positive plans) for nine box targets of 60 × 60 × 54 mm^3 at 0–280 mm depths in water. They were created with or without MLC, with 50–300 mm air gaps. The penumbra and average doses of MLC-positive and MLC-negative plans at the organs at risk (OAR) region of each box plan were compared. Besides, several plan doses were validated by measurements with penumbra (with an average of 80–20 % dose point widths for both side profiles) differences and 2D gamma analysis.

Results: The MLC-positive plans reduced the penumbra and mean OAR doses by 1.0–5.1 mm and 3.3–13.5 %, respectively, compared to MLC-negative plans even at >150 mm depths. The penumbra differences in measurements were <±1.5 mm for all plans. The mean gamma scores at 2 %/2 mm were 97.9 ± 2.3 % and 97.4 ± 3.1 % for the MLC-negative and MLC-positive plans, respectively.

Conclusions: The MLC-positive beams improved the penumbra and reduced the OAR dose in every depth region and air gap. We have shown that PBS with MLCs can be useful at more than 150 mm regions, depending on the machine.

1. Introduction

Proton pencil beam scanning (PBS) could irradiate the intensity-modulated beam by controlling several thousands of pencil beam spots, monitor units, and multiple energies [1,2]. PBS has better target conformity and better sparing of surrounding organs at risk (OAR) than photon therapy or passive scattering proton therapy (PSPT) [1,3]. However, the proton beam has a larger lateral penumbra than the photon beam, while the PBS plans may increase the dose to surrounding organs, as in PSPT plans, especially in shallow regions, due to the use of range shifters (RSs) [4–7]. Since there are more OARs in shallow treatment areas, such as the head and neck, than in deep treatment areas, a

* Corresponding author at: Department of Radiotherapy, Medical Co. Hakuhokai, Osaka Proton Therapy Clinic, 27-9 Kasugadenaka 1 Chome, Konohana-ku, Osaka, Osaka 554-0022, Japan.
E-mail address: yukitominaga1@gmail.com (Y. Tominaga).

https://doi.org/10.1016/j.ejmp.2025.105684
Received 22 October 2024; Received in revised form 13 July 2025; Accepted 28 November 2025
Available online 3 December 2025

clinical demand arises for treatment with the lowest possible lateral dose spread [8–10]. Several techniques have been proposed to improve lateral penumbra, including patient-specific aperture, dynamic collimation systems, and contour scanning [11–14].

Tominaga et al. reported new PBS beam commissioning results using a multileaf collimator (MLC), which is a collimation technique used in proton therapy [15]. The results of this validation were limited to one condition of air gap for several target sizes. In clinical practice, larger air gaps often occur due to arranged treatment angles and patient positioning [16]. In general, the agreement between measurements and Monte Carlo calculations does not deteriorate even for plans with large air gaps [17,18]. However, there are slight differences in the agreement between measurements and calculations for different air gaps [18]. These studies also did not include collimators, and measurement validation of different air gaps using our MLC was not reported.

Furthermore, no quantitative evaluation of penumbra improvement due to beams with MLC compared to without MLC was performed in this paper [15]. The penumbra widths deteriorate as the air gap increased for beams using RSs [18]. As such, the beam with an RS will increase the dose to the surrounding OARs more than a beam without an RS [19]. Although MLC should be used for a variety of diseases to reduce doses to the surrounding OARs as much as possible, the current consensus is that the limit of penumbra improvement by collimation for PBS devices with an MLC is up to 150 mm depth in water [20,21]. Although prior research results exist, proton beam machines with collimators have not yet been standardized, and different specifications may lead to different results [12,20,21]. Factors affecting the penumbra include spot size, source-to-axis distance (SAD), and nozzle structure, including collimators, and different results may be observed if the specifications are significantly different [12].

This study is a sequel to a previous study [15], and we specifically focused on the following issues in the above context. This study is a more detailed investigation of the characteristics of penumbra at various depths (including depths more than 150 mm) of the plans using the MLC and to validate the accuracy of the calculations for clinical use. Our unique machine has a very different specification from those of previous reports, and its validation will help to examine this issue from a more multifaceted perspective [12,15].

In this study, we first characterized the penumbra width variations with or without the MLC for all relevant parameters affecting the lateral penumbra: the energy range used, air gap, and presence or absence of RS. Furthermore, we also validated the dose calculation accuracy for these plans, which were improved with the lateral penumbra by modifying various parameters.

2. Methods

2.1. Proton therapy system

Our PBS machine was the MELTHEA V (Hitachi, Tokyo, Japan), equipped with a rotated gantry and a synchrotron that has a raster scanning method at the Medical Corporation, Hakuhokai, Osaka Proton Therapy Center (OPTC) [22]. The PBS system has 92 energy ranges (70.7–235.0 MeV), and the available water equivalent depth is 40–340 mm. The measured spot sizes (one sigma) in the air were 3.0–9.5 mm and 3.2–9.5 mm for the cross-line and in-line planes, respectively. To treat areas shallower than 40 mm, our machine used the RS with a water-equivalent length of at least 60 mm (minimum thickness of thick RS) [22]. Beam selection could be done both with- and without the MLC of PBS beams in the planning phase (Fig. 1). The MLC consisted of 54 pairs of collimators downstream of the treatment nozzle, which was made of iron with a thickness of 140 mm and leaf width of 3.75 mm (actual leaf width of the machine). MLC use in our system does not restrict the maximum field size compared to the beams without the MLC. The leaf width is determined by the maximum irradiation field. The distance between the isocenter and the MLC varies based on the position of the treatment nozzle, which ranges from 250 to 560 mm [22].

MLC is known to cause inter-leaf, intra-leaf, and leaf-end transmissions in both photon and proton therapy [23–25]. We also measured inter-leaf and leaf-end transmission based on the previous paper [24]. We created plans to irradiate a single spot of 235 MeV (maximum energy) at a depth of 20 mm. A plan was measured without MLC and with MLC fully closed at the isocenter plane (leaf-end transmission, Fig. 2a). Then, we measured a plan with the MLC closed using the ionization chamber (PinPoint 3D ion chamber, Type 31022; PTW) and the spot position was shifted 20 mm to the left (inter-leaf transmission, Fig. 2b). Measurements were taken at five points each for the open field and for the measurements in Figs. 2a and 2b, and were calculated based on the measured dose ratio of the two leaf transmissions to the open field.

2.2. Verification plans

Uniform dose plans were created using the RayStation 10A treatment planning system (TPS, RaySearch Laboratories, Stockholm, Sweden). Nine different targets in the 0–280 mm depth range (Fig. 3) were set up. The irradiation fields were 60 mm × 60 mm in size, and the target thickness in the depth direction (spread-out Bragg peak width) was 54 mm for all targets located at nine depths. Plans with the isocenter depths of 25 mm and 53 mm could only be created with RS because they included areas <40 mm (Table 1). The other seven depth plans were

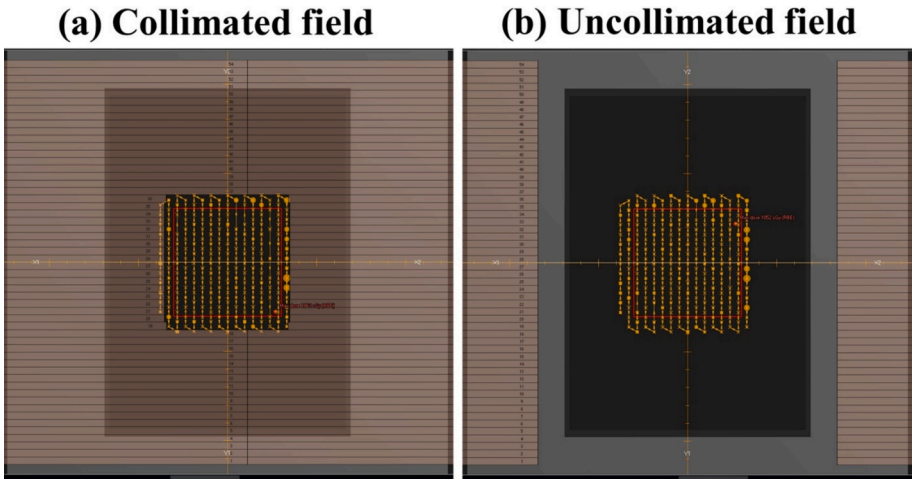

Fig. 1. Screenshots of the beam's eye view between the (a) collimated and (b) uncollimated fields with the same target volume (red contour). (For interpretation of the references to colour in this figure legend, the reader is referred to the web version of this article.)

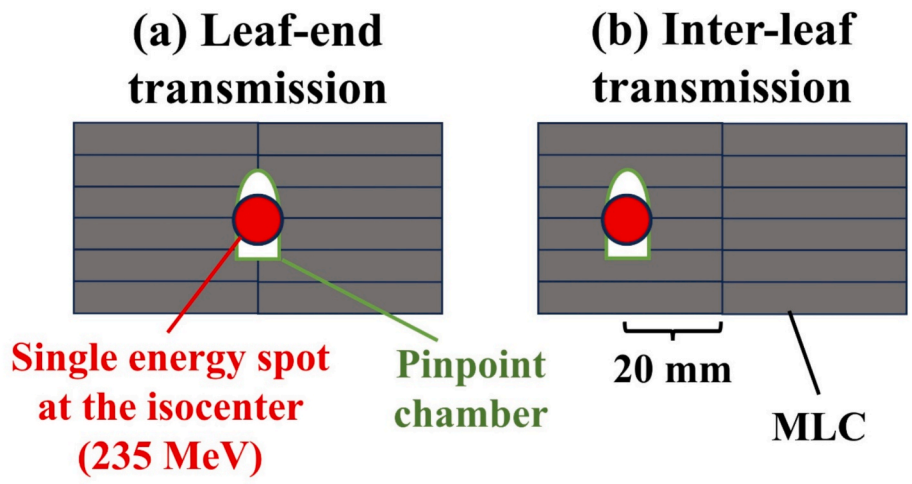

Fig. 2. Illustration of measurement conditions for (a) leaf-end transmission and (b) inter-leaf transmission.

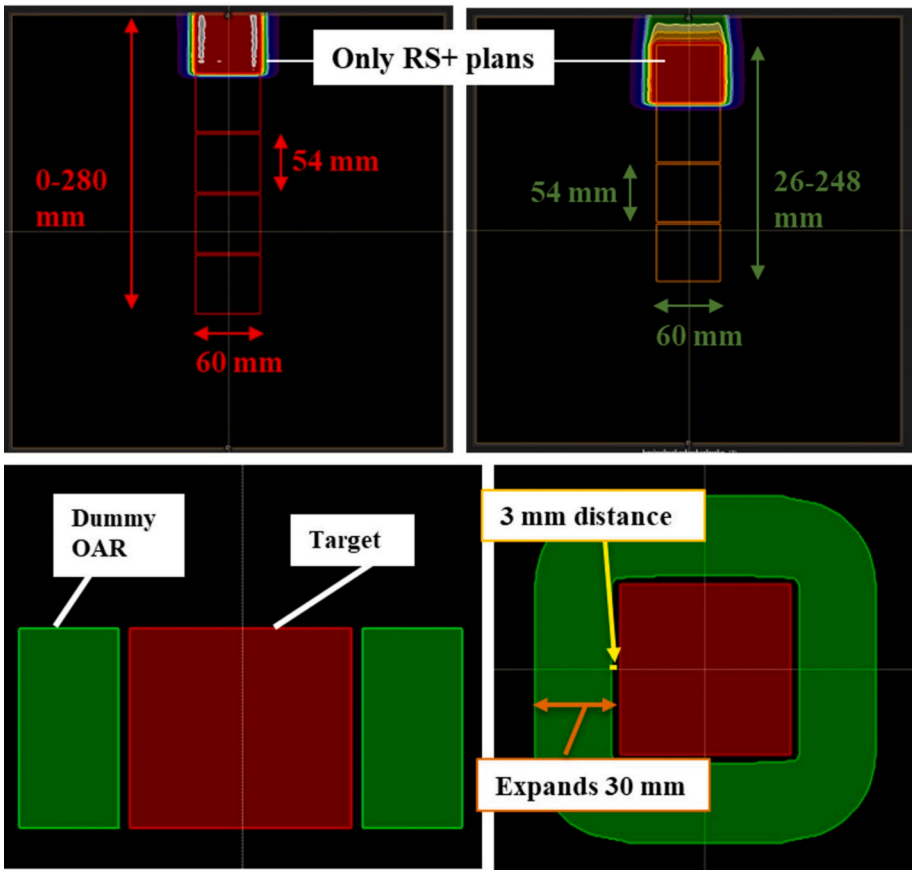

Fig. 3. Screenshots of the nine target definitions (upper row) and representative OAR definition (lower row) in the TPS. The large outer contour (brown) is the virtual water phantom with a volume of 400 × 400 × 400 mm^3, and the red and orange contours are the target contours with centers of gravity at various depths. Since the two contours with dose distributions inserted in the upper figure were located <40 mm regions, only plans with RS were created. OAR, Organ at risk; TPS, Treatment planning system; RS, Range shifters. (For interpretation of the references to colour in this figure legend, the reader is referred to the web version of this article.)

created both with- and without RS (RS-positive and RS-negative). In this study, RS was used even in areas deeper than 40 mm, where RS is usually not necessary. The reasons for this were based on studies that intentionally used a large spot size to reduce the interplay effect and also because we anticipated cases in which the isocenter would be deepened by a large target size placed on the surface [26]. Additionally, the use of RS has been reported to reduce irradiation time by reducing the number of spots and layers [27]. We investigated RS beams at all depths with the possibility of using such beams in clinical practice in the future. All plans were calculated using the same optimization conditions with air gap ranges of 50–300 mm at 50 mm intervals. However, some plans had limited air gaps because the treatment nozzle could only be set in the 250–560 mm range (Table 1). The reason for considering an air gap of up to 300 mm is that a treatment beam with such a large air gap might be

Table 1
Plan summary for 86 verification plans.

Isocenter depth (mm)	Target depth ranges (mm)	No range shifter plans			Range shifter plans		
		Air gaps (mm)	Energies (MeV)	Number of plans	Air gaps (mm)	Energies (MeV)	Number of plans
25	0–54	–	–	–	107.1*, 150, 200, 250, 300*	89.8–128.7	5
53	26–80	–	–	–	100*, 150, 200, 250, 300*	109.8–145.0	5
81	54–108	51.1*, 100, 150, 200, 250, 300*	86.4–126.5	6	51.1*, 100, 150, 200, 250, 300*	126.5–161.9	6
109	82–136	50*, 100, 150, 200, 250, 300*	106.6–143.1	6	50*, 100, 150, 200, 250, 300*	143.1–174.9	6
137	110–164	50*, 100, 150, 200, 250, 300*	124.5–157.6	6	50*, 100, 150, 200, 250, 300*	157.6–189.4	6
165	138–192	50*, 100, 150, 200, 250, 277.1*	141.2–172.6	6	50*, 100, 150, 200, 250, 277.1*	172.6–201.4	6
193	166–220	50*, 100, 150, 200, 249.1*	157.6–186.8	5	50*, 100, 150, 200, 249.1*	186.8–214.1	5
221	194–248	50*, 100, 150, 200, 222.1*	170.4–198.9	5	50*, 100, 150, 200, 222.1*	198.9–224.7	5
249	222–276	50*, 100, 150, 193.1*	184.4–201.4	4	50*, 100, 150, 193.1*	211.5–235.0	4

Air gaps, highlighted with an underline, and * mark are measured with a 2D array and film, respectively.

utilized when a clinical beam is assumed. For example, an air gap of about 300 mm can occur in situations where the patient's arm is raised above the torso while the treatment beam must be delivered from that direction. These consisted of 86 plans (38 and 48 patterns for the RS-negative and RS-positive plans, respectively), none of which used MLC (called uncollimated plans). Additionally, for all 86 plans, a plan with MLC was created with a 7.0 mm leaf margin in the isocenter plane (called collimated plans). This 7.0 mm leaf margin is clinically used by OPTC and was set as a leaf margin sufficient for all plans to achieve the target coverage. In the TPS, the collimator position is set first during optimization, and the spots are optimized while checking the collimator position. If the distance between the target and the MLC is close, the spot is placed so that the dose enters as evenly as possible within the limited irradiation field in the MLC to achieve coverage of the target limb in optimization. Therefore, the final spot position is determined by optimization, but in all layers, some of the spots outside of the irradiation field overlap with the MLC (Fig. 1a). When the MLC is used for PBS, the locations for spot placement in the optimization are strictly limited by the MLC. Spots can be positioned within a one sigma margin in air outside of the MLC's irradiation field. Consequently, spot placement may vary if the MLC margin is narrowed. With the 7.0 mm margin used in this study, most plans were developed without different spot placements.

The prescribed dose was 1.0 Gy at 98 % of the volume of each target for all plans. The calculation algorithm was a commercial Monte Carlo dose engine used in the TPS. Plan optimization and final dose calculation involved a particle number of 10,000 ions/spot and 0.5 % statistical uncertainty [22]. We defined penumbra widths as the 80–20 % dose points of the isocenter dose. In this study, the penumbra width was represented by the average of the widths on both sides.

The dose statistics from the dose-volume histograms (DVHs) for all box plans were compared between the collimated and uncollimated plans. Dummy OARs were created for all the plans. The dummy OARs were expanded by 30 mm in the lateral direction from the target and defined at a distance of 3 mm to avoid overlapping with the target (Fig. 3). The OAR dose statistics were compared between the mean (D_{mean}) and near-maximum (D_2) doses for the defined OARs at each isocenter depth, with the target coverage being identical at D_{98}. The $Dx_{\%}$ is indicated as the dose to x% volume of each structure.

We performed a statistical analysis on the improvement of penumbra width and OAR doses D_{mean} and D_2 at different air gaps. The statistical analysis was performed with a two-tailed Mann–Whitney *U* test using the Scipy package in Python. Comparisons were performed between collimated and uncollimated plans for different depth targets and with and without RS. We considered a p-value < 0.05 as statistically significant.

2.3. Measurements of 2D dose distributions

The 2D dose distributions in the isocenter plane were validated using a cross-calibrated OCTAVIUS Detector 729 (2D-array, PTW, Freiburg, Germany) and a solid water phantom (Tough Water; Kyoto Kagaku, Kyoto, Japan). The 2D array has 729 ionization chambers in a plane at 10 mm intervals, and the measurement procedure was the same as that in a previous study [15]. The plans with 50–107.1 mm (smallest), 150 mm, and 193.1–300 mm (largest) air gaps (three measurements per plan) of all air gap patterns were selected for our measurements, as highlighted (underlined) in Table 1. The measured doses were analyzed using gamma index analysis with an in-house analysis software based on the Pymedphys library [28]. The gamma criterion was set at 2 %/2 mm with a threshold of 90 % for the maximum dose. The purpose of this threshold analysis was to verify the dose distribution in uniform areas.

To validate the lateral penumbra widths with a higher resolution for both the collimated and uncollimated plans, additional measurements using a Gafchromic film (EBT4, Ashland Inc., Wayne, NJ, USA) were performed. Only the minimum and maximum air–gap plans for each target in both the RS-negative and RS-positive plans were measured (Table 1). The films were scanned with a scanner (EPSON DS-G20000, Seiko Epson Corp., Japan) at a resolution of 150 dots per inch (dpi). The lateral penumbra widths in the cross-line and in-line directions at the isocenter planes were compared between the measured and calculated 2D dose distributions using an in-house analysis software.

3. Results

3.1. Leaf transmission measurements

The average leakage doses from the two measurements were 0.21 ± 0.30 % and 0.07 ± 0.13 % for the leaf-end and inter-leaf transmissions, respectively. These leakage doses are lower than the results reported by Kang et al. [25]. Based on these results, the leakage dose generated by our MLC is as close to zero as possible.

3.2. Penumbra evaluations and 2D dose distribution validations

Fig. 4 and Table 2 show comparisons of the penumbra widths for the nine depth patterns between the collimated and uncollimated plans. Table 2 also shows the statistical analysis results. The penumbra widths

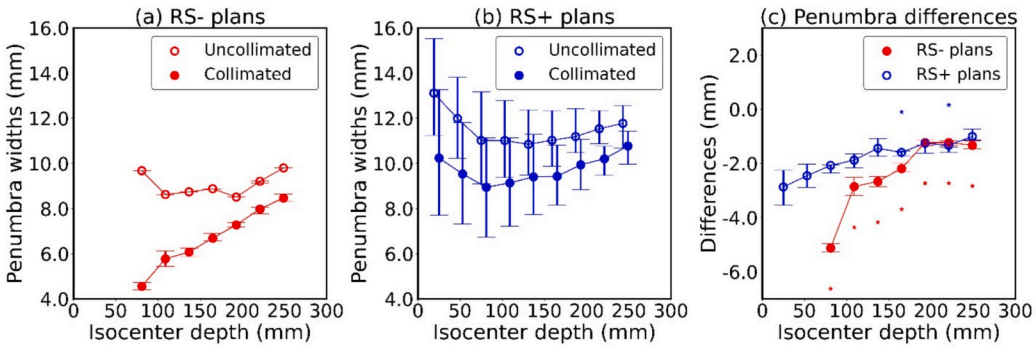

Fig. 4. Lateral penumbra width comparisons for (a) RS-negative plans and (b) RS-positive plans between the collimated and uncollimated plans, respectively. The (c) indicates the penumbra differences between the RS-negative (red color) and RS-positive (blue color) plans. The error bars in the Figures indicate the ranges of penumbra or penumbra differences from evaluated air gaps. RS, Range shifters; RS+, RS-positive; RS-, RS-negative. The * marks in the Fig. 4c mean statistically significant of p-value <0.05. (For interpretation of the references to colour in this figure legend, the reader is referred to the web version of this article.)

Table 2
Comparisons of penumbra widths for nine depth patterns between the collimated and uncollimated plans.

Isocenter depth (mm)	RS-negative plans (mm)				RS-positive plans (mm)			
	Collimated Av. ± SD	Uncollimated Av. ± SD	Difference Av. ± SD	p value	Collimated Av. ± SD	Uncollimated Av. ± SD	Difference Av. ± SD	p value
25	–	–	–	–	10.2 ± 2.0	13.1 ± 1.6	−2.9 ± 0.4	0.095
53	–	–	–	–	9.5 ± 1.6	12.0 ± 1.3	−2.5 ± 0.3	0.056
81	4.6 ± 0.1	9.7 ± 0.0	−5.1 ± 0.1	0.003 *	8.9 ± 1.5	11.0 ± 1.3	−2.1 ± 0.4	0.093
109	5.8 ± 0.2	8.6 ± 0.0	−2.9 ± 0.2	0.003 *	9.1 ± 1.4	11.0 ± 1.2	−1.9 ± 0.2	0.065
137	6.1 ± 0.1	8.7 ± 0.0	−2.7 ± 0.1	0.003 *	9.4 ± 1.2	10.8 ± 1.0	−1.4 ± 0.3	0.093
165	6.7 ± 0.1	8.9 ± 0.0	−2.2 ± 0.1	0.003 *	9.4 ± 0.9	11.0 ± 0.9	−1.6 ± 0.1	0.041 *
193	7.3 ± 0.1	8.5 ± 0.0	−1.2 ± 0.1	0.007 *	9.9 ± 0.8	11.2 ± 0.8	−1.3 ± 0.4	0.056
221	8.0 ± 0.1	9.2 ± 0.0	−1.2 ± 0.1	0.010 *	10.2 ± 0.5	11.5 ± 0.6	−1.3 ± 0.2	0.008 *
249	8.5 ± 0.1	9.8 ± 0.0	−1.3 ± 0.1	0.021 *	10.8 ± 0.5	11.8 ± 0.8	−1.0 ± 0.4	0.200

RS, Range shifters; Av. Average; SD, Standard deviation. The * marks in the table mean statistically significant of p-value < 0.05.

of collimated plans were improved at least by −1.2 ± 0.1 mm ($p < 0.05$ at 221 mm isocenter depth) and − 1.0 ± 0.4 mm ($p = 0.20$ at 249 mm isocenter depth) on average for RS-negative and RS-positive plans, respectively, compared to those of uncollimated plans. Further, the most improved average penumbra widths were −5.1 ± 0.1 mm ($p < 0.05$ at 81 mm isocenter depth) and −2.9 ± 0.4 mm ($p < 0.05$ at 25 mm isocenter depth) for RS-negative and RS-positive plans, respectively, both of which had the shallowest isocenter depths.

Table 3 compares the D_{mean} and D_2 OAR doses between the collimated and uncollimated plans. Table 3 also shows the statistical analysis results of both D_{mean} and D_2 OAR doses. The collimated plans could reduce D_{mean} on average by at least −3.3 ± 0.6 % ($p < 0.05$ at 193 mm isocenter depth) and −4.9 ± 0.7 % ($p = 0.151$ at 221 mm isocenter depth) for RS-negative and RS-positive plans, respectively, compared to

Table 3
Comparisons of mean and near-maximum OAR doses between the collimated and uncollimated plans.

Dose statistics	Isocenter depth (mm)	RS-negative plans (%)				RS-positive plans (%)			
		Collimated Av. ± SD	Uncollimated Av. ± SD	Difference Av. ± SD	p value	Collimated Av. ± SD	Uncollimated Av. ± SD	Difference Av. ± SD	p value
Mean doses (D_{mean})	25	–	–	–	–	24.5 ± 4.8	38.0 ± 6.3	−13.5 ± 1.8	0.016 *
	53	–	–	–	–	23.8 ± 4.1	35.3 ± 5.3	−11.5 ± 1.5	0.016 *
	81	17.0 ± 1.3	26.8 ± 0.0	−9.8 ± 1.3	0.003 *	22.8 ± 3.8	31.4 ± 4.7	−8.6 ± 1.4	0.015 *
	109	16.3 ± 1.1	21.5 ± 0.0	−5.2 ± 1.1	0.003 *	23.6 ± 4.0	31.3 ± 4.2	−7.7 ± 0.8	0.026 *
	137	17.1 ± 0.9	21.8 ± 0.0	−4.7 ± 0.9	0.003 *	24.3 ± 3.8	30.6 ± 4.5	−6.3 ± 1.4	0.093
	165	17.6 ± 0.5	21.4 ± 0.0	−3.8 ± 0.5	0.003 *	26.9 ± 4.1	32.6 ± 4.2	−5.8 ± 1.0	0.132
	193	18.9 ± 0.6	22.2 ± 0.0	−3.3 ± 0.6	0.007 *	25.7 ± 2.4	32.0 ± 2.6	−6.3 ± 0.6	0.016 *
	221	21.0 ± 0.5	25.8 ± 0.2	−4.8 ± 0.5	0.009 *	28.4 ± 3.1	33.3 ± 3.3	−4.9 ± 0.7	0.151
	249	22.8 ± 0.5	27.2 ± 0.0	−4.5 ± 0.5	0.020 *	28.0 ± 1.6	33.6 ± 3.1	−5.6 ± 1.6	0.029 *
Near-maximum doses (D_2)	25	–	–	–	–	89.3 ± 1.7	95.2 ± 1.5	−5.9 ± 0.7	0.008 *
	53	–	–	–	–	90.7 ± 1.2	95.7 ± 1.2	−4.9 ± 0.7	0.012 *
	81	94.1 ± 0.4	95.0 ± 0.0	−0.9 ± 0.4	0.003 *	91.3 ± 0.9	94.9 ± 0.8	−3.7 ± 1.3	0.005 *
	109	90.5 ± 0.4	91.7 ± 0.0	−1.2 ± 0.4	0.003 *	91.8 ± 1.1	95.2 ± 0.9	−3.5 ± 0.7	0.005 *
	137	91.6 ± 0.5	92.9 ± 0.0	−1.3 ± 0.5	0.003 *	92.0 ± 1.3	94.8 ± 1.6	−2.8 ± 0.8	0.037 *
	165	90.3 ± 0.5	90.8 ± 0.0	−0.5 ± 0.5	0.003 *	95.1 ± 2.9	96.0 ± 0.9	−0.9 ± 2.3	0.810
	193	90.8 ± 0.4	92.2 ± 0.0	−1.4 ± 0.4	0.007 *	92.2 ± 0.8	95.3 ± 0.4	−3.2 ± 0.5	0.012 *
	221	92.5 ± 0.3	94.9 ± 0.0	−2.4 ± 0.3	0.009 *	95.1 ± 2.2	95.0 ± 1.1	0.0 ± 1.3	0.753
	249	92.5 ± 0.5	94.8 ± 0.0	−2.3 ± 0.5	0.020 *	92.9 ± 0.4	96.0 ± 1.4	−3.1 ± 1.1	0.029 *

OAR, Organ at risk; RS, Range shifters; Av. Average; SD, Standard deviation. The percentage values in the table are defined as a percentage of the prescribed dose of 1.0 Gy. The * marks in the table mean statistically significant of p-value < 0.05.

uncollimated plans. Dose improvements were particularly pronounced for the 25 mm and 53 mm plans, both of which require the use of RS to achieve uniform irradiation. The D_{mean} and D_2 of these plans reduced the dose by at least −11.5 ± 1.5 % and −4.9 ± 0.7 % ($p < 0.05$ for both scenario), respectively, for 53 mm isocenter depth on average.

In the 2D-array measurements, the average gamma scores at 2 %/2 mm with a 90 % threshold (absolute dose evaluations) were 97.9 ± 2.3 % (90.6–100 %) and 97.4 ± 3.1 % (87.3–100 %) for the uncollimated and collimated plans, respectively. The gamma scores exceeded 90 % at 2 %/2 mm in all except five conditions for the collimated plans with the maximum air gap (Fig. 5).

Fig. 6 presents the representative film measurement results between the uncollimated and collimated plans. This plan has an isocenter depth of 137 mm, which is intermediate to the plan used in this study. The air gaps used for this measurement were 50 mm and 300 mm. The average (minimum/maximum) penumbra differences at the isocenter plane of all uncollimated plans were 0.44 ± 0.64 mm (−1.23/1.36 mm) and 0.82 ± 0.62 mm (−1.22/1.49 mm) for the cross-line and in-line profiles, respectively. The average (minimum/maximum) penumbra differences of all collimated plans were 0.23 ± 0.46 mm (−0.71/1.26 mm) and 0.34 ± 0.65 mm (−1.19/1.41 mm) for the cross-line and in-line profiles, respectively. All 72 penumbra widths (36 cross-line profiles and 36 in-line profiles) were within 1.5 mm. The results of our measurements showed agreement with the calculations regardless of the size of the air gap and whether collimators were used or not.

4. Discussions

In this study, the 2D dose distributions and penumbra widths between plans with- and those without MLC, as well as with or without RS for various air gaps, were evaluated and validated. To our knowledge, there is currently no other report on the evaluation of penumbra characteristics of MLC supported by MELTHEA V; hence, it is essential to investigate whether it shows a penumbra improvement trend similar to that in previous studies. The most important finding of this study is that the beam with MLC improved the penumbra even at depths more than 150 mm.

Our PBS beams with MLC improved the penumbra at depths up to 276 mm in water; this is deeper than the region where collimated beams generally improve the penumbra compared to beams without MLC [21,24]. Bues et al. found that with nickel's thin MLC, the boundary where the penumbra widths with- and that without the MLC coincide was 159 MeV (175 mm depth in water) [24]. Winterhalter et al. reported no improvement in the penumbra, even when collimators were placed in beams larger than 150 mm [21]. A similar consensus was observed for collimated PSPT beams and uncollimated PBS beams, as noted in the paper by Safai et al. [20]. Maes et al. reported that a PBS beam with a 65 mm brass aperture resulted in a penumbra reduction of <1 mm over an area >200 mm, which reduced the benefit of collimator use [29]. Additionally, the patient-specific aperture at the Nagoya Proton Therapy Center was designed initially to verify penumbra improvement only at depths up to 150 mm [11,30]. This is because the aperture was not designed to improve the penumbra in areas deeper than 150 mm (only a 30 mm thick brass aperture was supported) when the device was originally designed at this facility.

The possible reasons why our machine improved the collimator beam penumbra in deeper regions compared with those in previous studies are explained as follows. The first reason is the size of the beam spot in the air. Our machine had a beam size range of 3.0–9.5 mm. This is an intermediate beam size range compared to other treatment systems using collimators [12]. However, the one-sigma beam size of the device used in Winterhalter's paper [21], which showed no penumbra improvement over a 150 mm area, was approximately 2.3–5.0 mm in the 70–230 MeV range, significantly smaller than the size of the smaller machine used in this study [31]. If the original beam size is smaller, the collimated beam in air will enter a medium, such as water, with less improvement in the penumbra than the uncut beam. Since the lateral spread of the beam is mostly composed of a component due to its spread in water rather than in air, the small beam size cut in air would have resulted in little improvement due to the use of collimators. The second reason may be the large virtual SAD (VSAD) due to the equipment arrangement of the scanning magnets. The VSAD of our machine was 2696 mm and 3029 mm for the magnets in the X- and Y directions, respectively; these are larger than the VSADs of other treatment machines [13,20,31,32]. Charlwood et al. reported that collimation is less affected by penumbra reduction with shorter VSAD [33]. Our instrument has a larger VSAD than the hypothetical VSAD used in this study; thus, it is more affected. This study provides unprecedented and significant insight into the contribution of collimators to the improvement of penumbra depths greater than 150 mm. This information could have a significant impact on the future specification of proton beam system.

Generally, the main use of beams with collimators is limited to plans with RS at shallow depths. Notably, in this study, the improvement in the penumbra when collimators were used was greater for plans without RSs. As shown in Fig. 4c, in the range of 40–200 mm depth, the RS-negative plan with collimator showed an improvement of 1.2–5.1 mm (Table 2). Since the MLC, unlike the patient collimator, has no cost barrier to its use, the collimator should be used on all beams to improve the penumbra.

The current TPS dose calculations used in this study generally show worse measurement and calculation accuracies for plans with larger air gaps, collimators, and RSs as already found in the papers [15,17]. Some results below 90 % for gamma scores at 2 %/2 mm were observed mostly to targets present at depths <100 mm. This is similar to the results reported by Tominaga et al. [15]. This may be due to the presence of secondary particles generated by the MLC and RSs in the shallow region, not correctly reproduced by the TPS [34]. Furthermore, the deterioration in the gamma scores was limited to the largest air gap. An air gap of

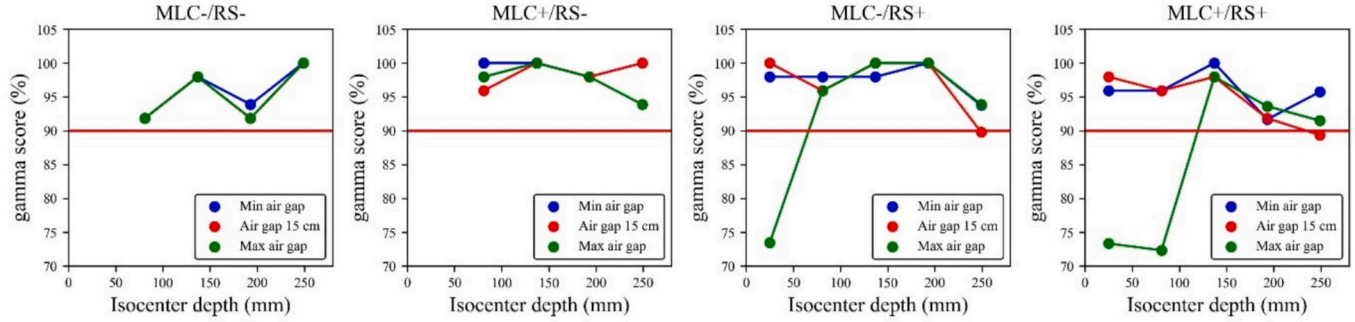

Fig. 5. Representative verification results between the 2D-array measurements and TPS doses in gamma analysis at 2 %/2 mm with a 90 % threshold. The two left and two right columns of the figure show plans without- and with RSs, respectively. TPS, Treatment planning system; RS, Range shifters; MLC, Multileaf collimator; min, minimum; max, maximum.

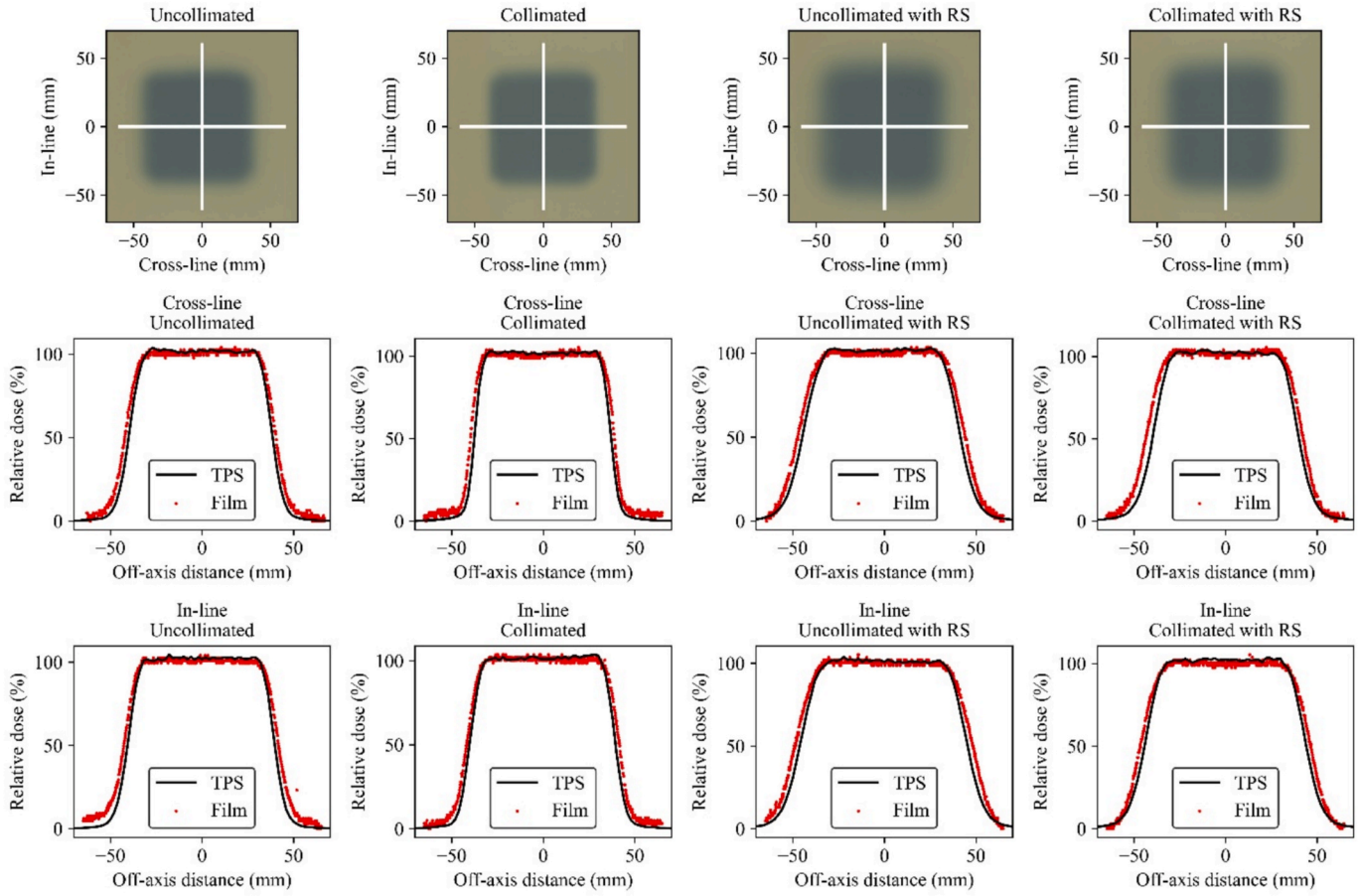

Fig. 6. Comparisons of film measurements (red scatter plots) and calculations (solid black lines) for uncollimated (first column), collimated (second column), uncollimated with RS (third column), and collimated with RS (fourth column) plans for a representative box target at the isocenter depth of 137 mm. TPS, Treatment planning system; RS, Range shifters. (For interpretation of the references to colour in this figure legend, the reader is referred to the web version of this article.)

300 mm is unlikely to be employed in shallow areas. Thus, it can be assumed that agreement between the measurement and calculation is ensured in the clinical use range.

The penumbra differences in film validations were all within ±1.5 mm at the smallest and largest air gaps, which is comparable to the results of another type of collimation machine validated in previous studies, which were also within ±1.5 mm [11,13]. Our results showed that the beams used in this study have good penumbra agreement at all depths, with or without collimators, and with or without RSs, regardless of the air gap size.

The OAR doses for the collimated beams were lower than those for the uncollimated beams for all box plans in terms of both the mean and maximum doses while maintaining target coverages. Our box plan's beams had a beam range of >200 mm, providing a treatment planning benefit for penumbra improvement even at treatment sites that cannot be improved beyond 150–200 mm, such as the machines used in the reports of Winterhalter et al. and Maes et al. [21,29]. The reduction in the mean dose to the OAR demonstrated the potential for a small reduction in the impact of late adverse effects. The disadvantage of using collimators is the generation of secondary neutrons [35]. Notably, RayStation's MC dose engine does not simulate secondary neutrons [36]. Therefore, the number of secondary neutrons generated in this study could not be determined. Although the use of collimators increases secondary neutron production, the treatment planning benefits of collimating the primary beam are thought to outweigh the risks of neutron exposure [35,37].

Slit scattering effects have also been reported in the past [38]. Slit scattering occurs when protons are deflected by the edges of slits or collimators used to shape the beam profile, resulting in unintended radiation outside the target area. This effect can introduce dose inaccuracies, particularly when high dosimetric precision is required, such as in the irradiation testing of electronic devices. Therefore, it is essential to consider and minimize slit scattering through careful collimator design and test setup.

This study has some limitations. This paper summarizes the penumbra improvements using single-field optimized plans. Intensity-modulated proton beam therapy beams that do not deliver a uniform dose to the target may result in minimal improvement of the penumbra. Furthermore, the smaller the margin between the target and MLC, the better the penumbra; however, the margin used in this study was only a clinically safe margin of 7.0 mm. If even smaller margins were used without sacrificing coverage, the difference between the uncollimated and collimated penumbrae would be greater. The optimal margin varies with the energy used (i.e., target depth), air gap, with and without RS, and target geometry. We plan to conduct a study of the optimal margin for each of these parameters while the target cover is not sacrificed in the future. Many optimal margin studies have been conducted not only in PBS but also in PSPT, and these findings should be considered in our MLC and PBS [20,24,39,40]. Further, research and development using dynamic collimation in this treatment system would be undertaken [41,42].

5. Conclusions

This study validated the 2D dose distributions and penumbra widths with or without MLC plans for various parameter changes, such as

energy ranges, air gaps, and RS with a thickness of 60 mm. Regardless of the use of RS, the collimated PBS beams could reduce the penumbra widths by 1.0–5.1 mm for all energy ranges. The collimated beams reduced both the mean and near-maximum doses of surrounding OARs than the uncollimated beams for both the RS-positive and RS-negative plans while maintaining target coverage. Although it has been a common theory that the effective range of a PBS beam with MLC is up to 150 mm, we have newly shown that this is not the case depending on the machine specifications.

Funding

This study was supported by JSPS KAKENHI (grant number: JP23K19590).

Declaration of competing interest

The authors declare that they have no known competing financial interests or personal relationships that could have appeared to influence the work reported in this paper.

Acknowledgments

The authors wish to thank the staff of the Osaka Proton Therapy Clinic for their cooperation in obtaining experimental data for the current study.

References

[1] Van De Water TA, Lomax AJ, Bijl HP, De Jong ME, Schilstra C, Hug EB, et al. Potential benefits of scanned intensity-modulated proton therapy versus advanced photon therapy with regard to sparing of the salivary glands in oropharyngeal cancer. Int J Radiat Oncol Biol Phys 2011;79:1216–24. https://doi.org/10.1016/j.ijrobp.2010.05.012.

[2] Lomax A. Intensity modulation methods for proton radiotherapy. Phys Med Biol 1999;44:185–205. https://doi.org/10.1088/0031-9155/44/1/014.

[3] Yoo GS, Il YJ, Cho S, Jung SH, Han Y, Park S, et al. Comparison of clinical outcomes between passive scattering versus pencil-beam scanning proton beam therapy for hepatocellular carcinoma. Radiother Oncol J Eur Soc Ther Radiol Oncol 2020;146:187–93. https://doi.org/10.1016/j.radonc.2020.02.019.

[4] Miyata J, Tominaga Y, Kondo K, Sonoda Y, Hanazawa H, Sakai M, et al. Dosimetric comparison of pencil beam scanning proton therapy with or without multi-leaf collimator versus volumetric-modulated arc therapy for treatment of malignant glioma off. J Am Assoc Med Dosim Med Dosim 2023;48:105–12. https://doi.org/10.1016/j.meddos.2023.01.008.

[5] St James S, Grassberger C, Lu H-M. Considerations when treating lung cancer with passive scatter or active scanning proton therapy. Transl Lung Cancer Res 2018;7:210–5. https://doi.org/10.21037/tlcr.2018.04.01.

[6] Saini J, Cao N, Bowen SR, Herrera M, Nicewonger D, Wong T, et al. Clinical commissioning of a pencil beam scanning treatment planning system for proton therapy. Int J Part Ther 2016;3:51–60. https://doi.org/10.14338/IJPT-16-0000.1.

[7] Bäumer C, Janson M, Timmermann B, Wulff J. Collimated proton pencil-beam scanning for superficial targets: impact of the order of range shifter and aperture. Phys Med Biol 2018;63:085020. https://doi.org/10.1088/1361-6560/aab79c.

[8] Righetto R, Fellin F, Scartoni D, Amichetti M, Schwarz M, Amelio D, et al. Is it beneficial to use apertures in proton radiosurgery with a scanning beam? A dosimetric comparison in neurinoma and meningioma patients. J Appl Clin Med Phys 2022;23:e13459. https://doi.org/10.1002/acm2.13459.

[9] Tominaga Y, Suga M, Takeda M, Yamamoto Y, Akagi T, Kato T, et al. Dose-volume comparisons of proton therapy for pencil beam scanning with and without multi-leaf collimator and passive scattering in patients with lung cancer off. J Am Assoc Med Dosim Med Dosim 2024;49:13–8. https://doi.org/10.1016/j.meddos.2023.10.006.

[10] Sugiyama S, Katsui K, Tominaga Y, Waki T, Katayama N, Matsuzaki H, et al. Dose distribution of intensity-modulated proton therapy with and without a multi-leaf collimator for the treatment of maxillary sinus cancer: a comparative effectiveness study. Radiat Oncol 2019;14. https://doi.org/10.1186/s13014-019-1405-y.

[11] Yasui K, Toshito T, Omachi C, Kibe Y, Hayashi K, Shibata H, et al. A patient-specific aperture system with an energy absorber for spot scanning proton beams: verification for clinical application. Med Phys 2015;42:6999–7010. https://doi.org/10.1118/1.4935528.

[12] Hyer DE, Bennett LC, Geoghegan TJ, Bues M, Smith BR. Innovations and the use of collimators in the delivery of pencil beam scanning proton therapy. Int J Part Ther 2021;8:73–83. https://doi.org/10.14338/IJPT-20-00039.1.

[13] Vilches-Freixas G, Unipan M, Rinaldi I, Martens J, Roijen E, Almeida IP, et al. Beam commissioning of the first compact proton therapy system with spot scanning and dynamic field collimation. Br J Radiol 2020;93:20190598. https://doi.org/10.1259/bjr.20190598.

[14] Meier G, Leiser D, Besson R, Mayor A, Safai S, Weber DC, et al. Contour scanning for penumbra improvement in pencil beam scanned proton therapy. Phys Med Biol 2017;62:2398–416. https://doi.org/10.1088/1361-6560/aa5dde.

[15] Tominaga Y, Sakurai Y, Miyata J, Harada S, Akagi T, Oita M. Validation of pencil beam scanning proton therapy with multi-leaf collimator calculated by a commercial Monte Carlo dose engine. J Appl Clin Med Phys 2022;23. https://doi.org/10.1002/acm2.13817.

[16] Saini J, Traneus E, Maes D, Regmi R, Bowen SR, Bloch C, et al. Advanced proton beam dosimetry part I: review and performance evaluation of dose calculation algorithms. Transl Lung Cancer Res 2018;7:171–9. https://doi.org/10.21037/tlcr.2018.04.05.

[17] Saini J, Maes D, Egan A, Bowen SR, St James S, Janson M, et al. Dosimetric evaluation of a commercial proton spot scanning Monte-Carlo dose algorithm: comparisons against measurements and simulations. Phys Med Biol 2017;62:7659–81. https://doi.org/10.1088/1361-6560/aa82a5.

[18] Shirey RJ, Wu HT. Quantifying the effect of air gap, depth, and range shifter thickness on TPS dosimetric accuracy in superficial PBS proton therapy. J Appl Clin Med Phys 2018;19:164–73. https://doi.org/10.1002/acm2.12241.

[19] Huang S, Kang M, Souris K, Ainsley C, Solberg TD, McDonough JE, et al. Validation and clinical implementation of an accurate Monte Carlo code for pencil beam scanning proton therapy. J Appl Clin Med Phys 2018;19:558–72. https://doi.org/10.1002/acm2.12420.

[20] Safai S, Bortfeld T, Engelsman M. Comparison between the lateral penumbra of a collimated double-scattered beam and uncollimated scanning beam in proton radiotherapy. Phys Med Biol 2008;53:1729–50. https://doi.org/10.1088/0031-9155/53/6/016.

[21] Winterhalter C, Meier G, Oxley D, Weber DC, Lomax AJ, Safai S. Contour scanning, multi-leaf collimation and the combination thereof for proton pencil beam scanning. Phys Med Biol 2018;64:015002. https://doi.org/10.1088/1361-6560/aaf2e8.

[22] Tominaga Y, Oita M, Akagi T, Miyata J, Harada S, Matsuda T, et al. Comparison of the dose calculation accuracy between the commercial pencil beam algorithm and various statistical uncertainties with Monte Carlo algorithm in new proton pencil beam scanning system. Radiat Environ Med 2023;12:53–64. https://doi.org/10.51083/radiatenvironmed.12.1_53.

[23] Boyer A, Biggs P, Galvin J, Klein E, LoSasso T, Low D, et al. AAPM report 72-basic applications of Multileaf collimators. Med Phys 2001;72:1–54. https://doi.org/10.37206/71.

[24] Bues M, Newhauser WD, Titt U, Smith AR. Therapeutic step and shoot proton beam spot-scanning with a multi-leaf collimator: a Monte Carlo study. Radiat Prot Dosim 2005;115:164–9. https://doi.org/10.1093/rpd/nci259.

[25] Kang M, Pang D. Commissioning and beam characterization of the first gantry-mounted accelerator pencil beam scanning proton system. Med Phys 2020;47:3496–510. https://doi.org/10.1002/mp.13972.

[26] Grassberger C, Dowdell S, Sharp G, Paganetti H. Motion mitigation for lung cancer patients treated with active scanning proton therapy. Med Phys 2015;42:2462–9. https://doi.org/10.1118/1.4916662.

[27] Liu C, Schild SE, Chang JY, Liao Z, Korte S, Shen J, et al. Impact of spot size and spacing on the quality of robustly optimized intensity modulated proton therapy plans for lung cancer. Int J Radiat Oncol Biol Phys 2018;101:479–89. https://doi.org/10.1016/j.ijrobp.2018.02.009.

[28] Guterres Marmitt G, Pin A, Ng Wei Siang K, Janssens G, Souris K, Cohilis M, et al. Platform for automatic patient quality assurance via Monte Carlo simulations in proton therapy. Phys Med 2020;70:49–57. https://doi.org/10.1016/j.ejmp.2019.12.018.

[29] Maes D, Regmi R, Taddei P, Bloch C, Bowen S. Parametric characterization of penumbra reduction for aperture-collimated pencil beam scanning (PBS) proton therapy collimated pencil beam scanning (PBS) proton therapy. Biomed Phys Eng Express 2019;5:035002. https://doi.org/10.1088/2057-1976/ab0953.

[30] Yasui K, Toshito T, Omachi C, Hayashi K, Tanaka K, Asai K, et al. Evaluation of dosimetric advantages of using patient-specific aperture system with intensity-modulated proton therapy for the shallow depth tumor. J Appl Clin Med Phys 2018;19:132–7. https://doi.org/10.1002/acm2.12231.

[31] Safai S, Bula C, Meer D, Pedroni E. Improving the precision and performance of proton pencil beam scanning. Transl Cancer Res (Particle Beam Ther I) 2012;3:2012. https://tcr.amegroups.org/article/view/599/html.

[32] Langner UW, Eley JG, Dong L, Langen K. Comparison of multi-institutional Varian ProBeam pencil beam scanning proton beam commissioning data. J Appl Clin Med Phys 2017;18:96–107. https://doi.org/10.1002/acm2.12078.

[33] Charlwood FC, Aitkenhead AH, MacKay RI. A Monte Carlo study on the collimation of pencil beam scanning proton therapy beams. Med Phys 2016;43:1462–72. https://doi.org/10.1118/1.4941957.

[34] RaySearch Laboratory. RayStation 10A reference manual. 2020.

[35] Kim DH, Park S, Jo K, Cho S, Shin EH, Lim DH, et al. Investigations of line scanning proton therapy with dynamic multi-leaf collimator. Phys Medica 2018;55:47–55. https://doi.org/10.1016/j.ejmp.2018.10.009.

[36] Bäumer C, Plaude S, Khalil DA, Geismar D, Kramer P-H, Kröninger K, et al. Clinical implementation of proton therapy using pencil-beam scanning delivery combined with static apertures. Front Oncol 2021;11:599018. https://doi.org/10.3389/fonc.2021.599018.

[37] Iwata H, Toshito T, Hayashi K, Yamada M, Omachi C, Nakajima K, et al. Proton therapy for non-squamous cell carcinoma of the head and neck: planning comparison and toxicity. J Radiat Res 2019;60:612–21. https://doi.org/10.1093/jrr/rrz036.

[38] McMahan MA, Blackmore E, Cascio EW, Castaneda C, von Przewoski B, Eisen H, et al. IEEE radiation effects data workshop. New York: IEEE 2008;2008:135–41. https://doi.org/10.1109/REDW.2008.31.
[39] Gottschalk B. Multileaf collimators, air gap, lateral penumbra, and range compensation in proton radiotherapy. Med Phys 2011;38:i–ii. https://doi.org/10.1118/1.3653297.
[40] Kimstrand P, Traneus E, Ahnesjö A, Tilly N. Parametrization and application of scatter kernels for modelling scanned proton beam collimator scatter dose. Phys Med Biol 2008;53:3405–29. https://doi.org/10.1088/0031-9155/53/13/001.
[41] Smith BR, Hyer DE, Culberson WS. An investigation into the robustness of dynamically collimated proton therapy treatments. Med Phys 2020;47:3545–53. https://doi.org/10.1002/mp.14208.
[42] Grewal HS, Ahmad S, Jin H. Performance evaluation of adaptive aperture's static and dynamic collimation in a compact pencil beam scanning proton therapy system: a dosimetric comparison study for multiple disease sites. Med Dosim 2021; 46:179–87. https://doi.org/10.1016/j.meddos.2020.11.001.